

Img-Diff: Contrastive Data Synthesis for Multimodal Large Language Models

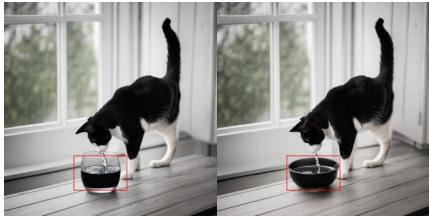
Qirui Jiao
Sun Yat-sen University
Shenzhen, Guangdong, China
jiaoqr3@mail2.sysu.edu.cn

Daoyuan Chen
Alibaba Group
Hangzhou, Zhejiang, China
daoyuanchen.cdy@alibaba-inc.com

Yilun Huang
Alibaba Group
Hangzhou, Zhejiang, China
lielin.hyl@alibaba-inc.com

Yaliang Li
Alibaba Group
Bellevue, Washington, United States
yaliang.li@alibaba-inc.com

Ying Shen
Sun Yat-sen University
Shenzhen, Guangdong, China
sheny76@mail.sysu.edu.cn



The left image shows a cat drinking water from a **glass**, while the right image shows the same cat drinking water from a **black bowl**. The difference is the type of container used for the water.



The difference between the two images lies in the object that the player is holding. In the left image, the player is holding a **baseball glove**, while in the right image, the player is holding a **basketball**.



The left image shows a **framed picture** on a shelf, while the right image shows a **white vase with pink flowers**. The difference is that the left image has a framed picture, while the right image has a vase with flowers.

Figure 1: Examples of generated “object replacement” data within IMG-DIFF.

Abstract

High-performance Multimodal Large Language Models (MLLMs) rely heavily on data quality. This study introduces a novel dataset named Img-Diff, designed to enhance fine-grained image recognition in MLLMs by leveraging insights from contrastive learning and image difference captioning. By analyzing object differences between similar images, we challenge models to identify both matching and distinct components. We utilize the Stable-Diffusion-XL model and advanced image editing techniques to create pairs of similar images that highlight object replacements. Our methodology includes a Difference Area Generator for object differences identifying, followed by a Difference Captions Generator for detailed difference descriptions. The result is a relatively small but high-quality dataset of “object replacement” samples. We use the proposed dataset to finetune state-of-the-art (SOTA) MLLMs such as MGM-7B, yielding comprehensive improvements of performance scores over SOTA models that trained with larger-scale datasets, in numerous image difference and Visual Question Answering tasks. For instance, our trained models notably surpass the SOTA models GPT-4V and Gemini on the MMVP benchmark. Besides, we investigate alternative methods for generating image difference data through “object removal” and conduct thorough evaluation to confirm the dataset’s diversity, quality, and robustness, presenting several insights on synthesis of such contrastive dataset. To encourage further research and advance the field of

multimodal data synthesis and enhancement of MLLMs’ fundamental capabilities for image understanding, we release our codes and dataset at <https://github.com/modelscope/data-juicer/tree/ImgDiff>.

1 Introduction

The emergence of large language models (LLMs) has revolutionized natural language processing (NLP) [45, 60]. This advancement has paved the way for the development of Multimodal Large Language Models (MLLMs) that seamlessly integrate linguistic and visual understanding. Improving the performance of MLLMs hinges on two primary avenues: evolving model architectures and enhancing dataset quality. The majority of state-of-the-art MLLMs [3, 35, 39–41] implement a two-phase approach, commencing with a pre-training phase involving extensive image-text pairs for modality alignment, followed by fine-tuning aimed at optimizing visual question answering (VQA) capabilities with specific instruction tuning datasets.

The efficacy of pretraining datasets profoundly affects MLLMs’ capabilities in performing core visual tasks. Concurrently, the quality of visual instruction tuning datasets plays a crucial role in the overall performance of MLLMs in VQA tasks and diverse downstream applications. With the evolution of visual instruction tuning datasets, several recent studies have successfully integrated object detection and Optical Character Recognition (OCR) datasets, such as Refcoco [26], Visual Genome [29], OCR-VQA [46], and TextVQA

[56], significantly enhancing MLLMs’ proficiency in tasks requiring detailed image perception.

In light of advancements in contrastive learning and image difference captioning research in specific domains [5, 23, 48], which underscores the potential of pair of different images in refining models’ image recognition capabilities, we introduce a general-purpose yet challenging dataset named IMG-DIFF. This novel dataset sets itself apart from existing visual instruction tuning datasets by generating pairs of very similar images featuring subtle object alterations. Rather than compelling MLLMs to focus solely on a single image, our dataset challenges them to analyze paired images and articulate the differences within designated regions. By doing so, we aim to empower MLLMs with enhanced abilities to scrutinize intricate areas within images and assess discrepancies across corresponding regions, thereby augmenting their fine-grained image recognition capabilities.

Following the construction of our dataset, we integrate it into the original visual instruction tuning datasets of LLaVA-1.5 [39] and MGM [35]. Subsequently, we perform fine-tuning on these models and evaluate their performance on image difference benchmarks, including MMVP [59], Spot-the-Diff [23], and Image-Edit-Request [58], as well as widely recognized MLLM benchmarks. Our evaluation results reveal that after fine-tuning with our IMG-DIFF dataset, LLaVA-1.5-7B and MGM-7B achieve notable enhancements in image difference benchmarks, aligning their performance with state-of-the-art (SOTA) models. For instance, they notably surpass the SOTA models GPT-4V[1] and Gemini[13] on the MMVP benchmark. Moreover, these models exhibit comprehensive improvements across numerous well-recognized MLLM benchmarks, achieving an average score improvement of up to 3.06%, underscoring the useful role our dataset plays in bolstering MLLMs’ competencies in both image difference recognition and fine-grained image analysis.

We further evaluate the diversity and quality of our dataset, ensuring it encompasses a broad array of object categories while showcasing rich variability. Through meticulous manual labeling, we affirm the high quality of the dataset. Additionally, we conduct ablation studies to examine the effects of various filtering intensities. We also investigate an alternative methodology for constructing image difference data focused on “object removal”, assessing its effectiveness on LLaVA-1.5-7B and MGM-7B, and present fruitful insights on construction of contrastive data synthesis.

Our contributions are summarized as follows:

- We present a novel data synthesis method and an effect-proven IMG-DIFF dataset, comprising pairs of very similar images generated through object replacement, with a focus on processes such as segmentation, filtering, and detailed captioning of image difference .
- We execute visual instruction tuning on LLaVA-1.5-7B and MGM-7B using our dataset, and rigorously assess the fine-tuned models’ performance on many image difference benchmarks and widely-used MLLM benchmarks, demonstrating substantial performance improvements.
- We provide a comprehensive evaluation of the diversity and quality of the proposed dataset, confirming its richness and high standard. Through ablation studies, we identify empirical good filtering thresholds for such contrastive dataset.

- We open-source our dataset and codes at () to facilitate ongoing research, encouraging innovative endeavors in more MLLM datasets and image difference methodologies.

2 Background and Related Works

2.1 Multimodal Large Language Models

Multimodal Large Language Models (MLLMs) have exhibited remarkable advancements since their introduction. Research highlights two key factors that primarily influence the effectiveness of MLLMs: model architecture and dataset quality [50].

With respect to model architecture, notable approaches include Flamingo [2], IDEFICS [22, 30], BLIP-2 [32], and Qwen-VL [3], which leverage learnable queries to extract essential information from the CLIP [12, 51] image features. Alternatively, LLaVA [39–41] and MGM [35] utilize projection-based interfaces to facilitate interactions between text and image modalities. Furthermore, LLaMA-Adapter [70] and LaVIN [44] implement parameter-efficient tuning mechanisms to transfer image-related information to the LLM. A recent work also show usefulness of object detection model for MLLMs [24].

From the perspective of datasets, there are two prevalent strategies: enhancing the quality of pretraining data and improving visual instruction tuning data. The former aims for better semantic alignment between images and text by introducing substantial numbers of image-text pairs, enabling MLLMs to proficiently address fundamental visual tasks, such as image captioning. However, MLLMs trained exclusively on pretraining datasets may encounter difficulties with VQA challenges. Recent research has increasingly concentrated on refining visual instruction tuning datasets, enabling MLLMs to enhance performance across diverse question-answering tasks. Works like LLaVA [39–41], InstructBLIP [11], SPHINX [38], and MGM [35] leverage high-quality finetuning datasets characterized by extensive task diversity, allowing models to excel in tasks related to image perception, reasoning, and optical character recognition (OCR). Additionally, methods such as Shikra [9], ASM [66], and PINK [67] utilize substantial amounts of object detection data to enhance the models’ localization capabilities.

In contrast to previous works, our research introduces a dataset that emphasizes image differences, showing empirical effectiveness and great potential to augment MLLMs’ VQA proficiency, object localization capabilities, and discernment of image distinctions.

2.2 Datasets on Image Differences

Datasets focused on image differences typically consist of pairs of similar images supplemented with textual descriptions of their variations. For instance, the Spot-the-Diff dataset [23] contains pairs of street scenes captured at different times by the same surveillance cameras. The CLEVR-Change dataset [48] delineates scene variations of geometric objects against a clean backdrop. The Birds-to-Words dataset [65] elaborates on the nuanced differences among various bird species found in natural habitats. The Image-Edit-Request [58] dataset features edited images alongside their original counterparts, accompanied by descriptions of the modifications made.

Leveraging advancements in image editing technologies, some studies have employed generative models and editing techniques to

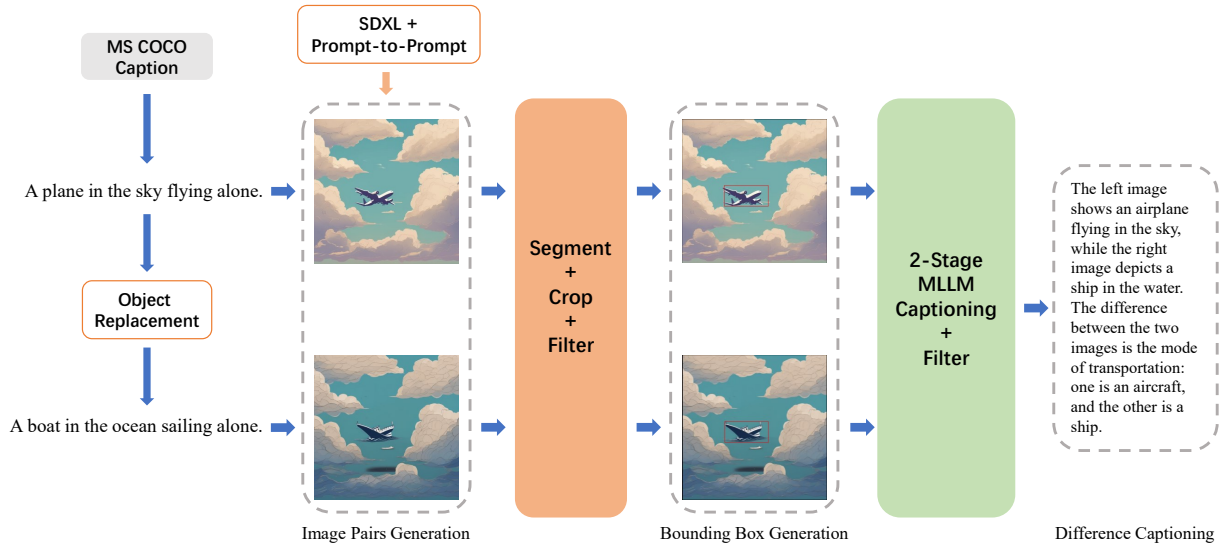


Figure 2: An overview of the generation process for “object replacement” data.

create datasets centered on image differences. A prime example is InstructPix2Pix [6], which utilizes the Prompt-to-Prompt [17] image editing technique to direct Stable-Diffusion-1.5 [52] in generating pairs of similar images, while employing GPT-3 [45] to craft the edited text as reference captions for image differences.

Our approach, similar to InstructPix2Pix, employs the Prompt-to-Prompt technique alongside a generative model Stable-Diffusion-XL [49] to generate pairs of similar images. However, we incorporate multiple filtering stages to ensure data quality, with a particular emphasis on producing difference captions that focus on specific bounding box regions rather than the entire image, which ensures greater accuracy.

2.3 Models for Image Difference Captioning

Image Difference Captioning (IDC) represents a specialized domain within image captioning characterized by its focus on subtle variations between images, rather than merely identifying common objects. The pioneering work in IDC, Spot-the-Diff [23], suggests potential change clusters and employs an LSTM [18] decoder to generate captions addressing these variations. DUDA [48] explores image differences at the semantic level using ResNet [16] and an LSTM to compute dynamic attention weights, producing captions that accurately depict these differences. VARD [61] introduces a viewpoint-adaptive representation disentanglement network based on LSTM for differentiating between real and pseudo changes. Meanwhile, NCT [62] employs a transformer [63] to integrate neighboring features, and CLIP4IDC [15] uses BERT-like training methodologies, adapting a CLIP model for IDC tasks.

With the emergence of MLLMs, VIXEN [5] marks the inaugural use of these models for IDC tasks, attempting to extract features from CLIP outputs using linear layers or Q-formers and subsequently concatenating the features of differential images for input into an LLM to generate image difference captions.

In contrast, our dataset is specifically designed for MLLMs. We construct our data based on the visual instruction tuning format established by mainstream MLLMs like LLaVA-1.5 and MGM, highlighting a new direction for exploration aimed at enhancing MLLMs from a data-centric perspective.

3 The Curation of IMG-DIFF

3.1 Overview

In recent years, contrastive learning methods have significantly improved the image-text understanding of vision-language models [51]. These methods involve repeatedly pairing batches of images and texts, requiring the model to distinguish between matching and non-matching image-text pairs, which enhances the model’s capability to differentiate between semantically similar and dissimilar image-text pairs. Our method incorporates contrastive learning principles and applies them to generate MLLM image-text data. Specifically, our method focuses on replacing objects between the image pairs, requiring MLLMs to identify similarities and differences in specific areas of the images, which aims to improve MLLMs’ abilities to recognize fine-grained differences in images.

The process of generating “object replacement” data can be divided into three parts. The first part is to generate similar images and form image pairs, where the only difference between these pairs are object replacement. Next, we name the second part “Difference Area Generator”, which extracts bounding box regions containing object differences between the image pairs. The third part, called the “Difference Captions Generator”, uses an MLLM to generate descriptive text for the areas containing object differences and then create question-answer pairs with questions such as “What objects have changed in this area?”. The process involves many model selections, which are discussed in Appendix B.2. The process also involves multiple filtering operations, with the specific thresholds

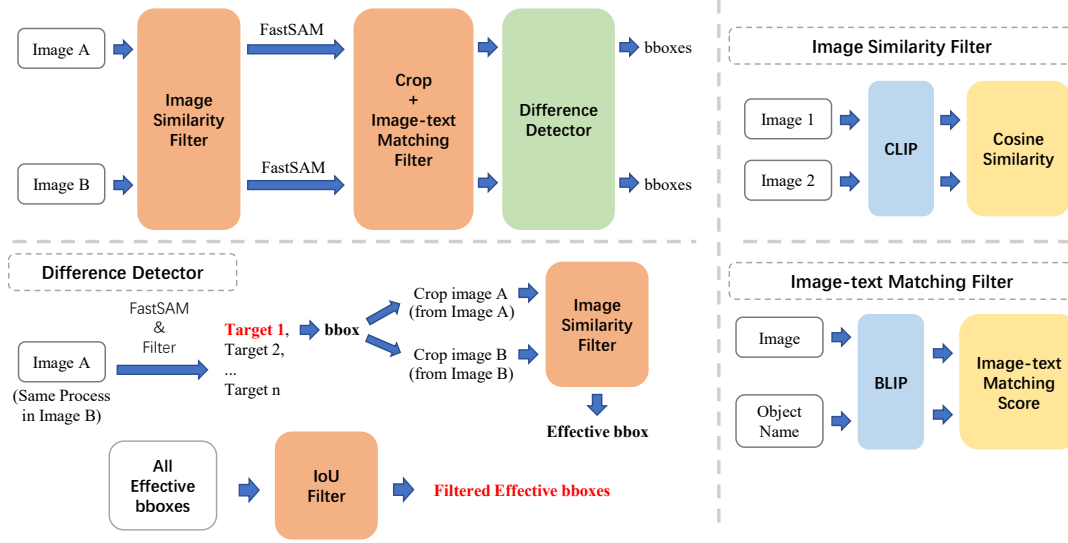


Figure 3: An overview of the Difference Area Generator and its three internal components: Image Similarity Filter, Image-text Matching Filter, and Difference Detector.

detailed in Appendix B.3, which we determine through experimental comparisons in Section 4.6. The sample examples are presented in Appendix C. The general framework is shown in Figure 2. To enhance the reproducibility and reusability, our proposed components and the end-to-end construction pipeline are implemented as data processing operators and configurable data recipes of Data-Juicer [7, 8] respectively.

3.2 Image Pairs Generation

Before generating the IMG-DIFF data, we first need to generate numerous pairs of similar images. The process is shown in Figure 2, which involves replacing the objects in images. We refer to InstructPix2Pix[6] and employ a generative model combined with image editing techniques to generate image pairs. However, while InstructPix2Pix utilizes the Stable-Diffusion-1.5, we use the more advanced Stable-Diffusion-XL[49] to produce more realistic images.

We start by obtaining 118K image captions from MS COCO[37], which are descriptions biased towards real photos. Then, we use the LLM Vicuna-1.5-13B[10] to perform object replacement in the captions. The prompt used is “Here is a sentence: ‘INPUT’. Please only replace one of the objects in this sentence with another object.” Here, INPUT refers to the original caption, and the answers from the LLM are the new captions. Finally, based on the caption pairs, we use the text-to-image generative model Stable-Diffusion-XL and image editing technique Prompt-to-Prompt[17] to generate image pairs with only few objects replaced.

3.3 Difference Area Generator

3.3.1 Overview. The Difference Area Generator aims to identify the locations of object differences between the image pair. Although object detection models are capable of identifying objects inside

images, the range of object categories is quite limited[25, 69]. Therefore, to increase the number of detectable object categories and enhance dataset diversity, we develop the Difference Area Generator based on segmentation and image similarity comparisons. The process is illustrated in Figure 3.

In this phase, we first use the Image Similarity Filter to obtain image pairs with high similarity but not completely identical and use FastSAM[71] to perform image segmentation on each image. Next, we crop the images based on the bounding box information got from segmentation and use the Image-text Matching Filter to filter the cropped sub-images for the presence of valid objects. Finally, we use the Difference Detector to determine whether there are indeed differences between the bounding box regions of the image pairs and perform IoU (Intersection over Union) filtering to remove overlapping bounding boxes, ultimately obtaining valid bounding box information.

3.3.2 Image Similarity Filter. The Image Similarity Filter aims to filter image pairs based on the degree of similarity. The module first uses CLIP[51] to extract image features from each image in the image pair and then calculates the cosine similarity. If their cosine similarity falls within the pre-set threshold, the image pair will be considered valid. We use the Image Similarity Filter twice in the Difference Area Generator. At the beginning stage, before using FastSAM for segmentation, we use the module to ensure that the image pairs are highly similar but not exactly the same. In the Difference Detector stage, after cropping sub-images based on the bounding box information, we use the module to filter the sub-image pairs and keep only the differing ones.

3.3.3 Image-text Matching Filter. The Image-text Matching Filter determines whether an image contains valid objects (i.e., the replaced or replacing objects). This module first uses BLIP[33] to

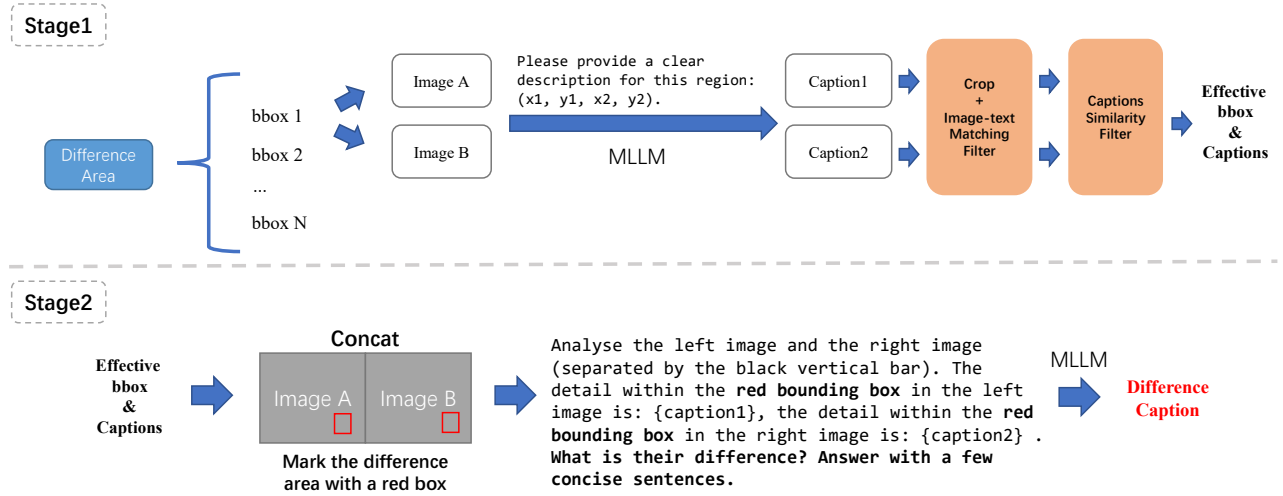


Figure 4: An overview of the Difference Captions Generator and its two stages.

extract image features, which are then compared with textual features of object names. When the image-text matching score falls within the pre-set threshold, we consider the image to contain valid objects. In the mid-stage of the Difference Area Generator, after performing sub-image cropping based on the bounding box information, we use the module to determine whether these sub-images contain valid objects and get valid bounding boxes.

3.3.4 Difference Detector. The Difference Detector is used in the final stage of the Difference Area Generator. This module determines whether there are differences between the bounding box regions of the image pair. For a given bounding box, we first crop two sub-images from both image A and B based on it. These two sub-images are then filtered through the Image Similarity Filter and the bounding box is considered effective only if the difference is significant enough. After processing all bounding boxes, we use the IoU method to filter out overlapping bounding boxes. Only the bounding boxes with a higher degree of difference are retained. The remaining bounding boxes are the effective bounding boxes ultimately outputted by the Difference Area Generator.

3.4 Difference Captions Generator

3.4.1 Overview. After obtaining the valid bounding box regions, we use the Difference Captions Generator to generate difference captions about the content of these regions (with each round of process focusing on only one bounding box in one image pair). The reason our difference captions only target specific regions is that an image pair can contain multiple object differences and a single difference caption cannot fully capture all of them. Therefore, we highlight specific regions with red boxes and provide targeted difference captions to ensure greater accuracy.

The module consists of two stages: the first stage generates content captions for the bounding box regions and then filters the bounding boxes with these generated captions using the Image-text Matching Filter and the Captions Similarity Filter. The second

stage uses the content captions and the images highlighted with red boxes to generate difference captions. The overview process is shown in Figure 4.

3.4.2 Stage1: Object Labeling & Filter. In Stage1, for each image pair, we first select N bounding box regions with the lowest similarity between images (N is set to 5 in this project) as candidate regions. Then, for each bounding box, we use the MLLM LLaVA-NEXT[40] to describe its corresponding regions and then apply two filtering processes: the first filter is the Image-text Matching Filter, which checks whether the content of the regions matches the captions; the second filter is the Captions Similarity Filter, which assesses whether there are differences between the two captions. Once the filtering is complete, we obtain valid bounding boxes and captions for subsequent difference captioning.

3.4.3 Captions Similarity Filter. The Captions Similarity Filter determines whether the two captions corresponding to the same bounding box coordinate are different. We use CLIP to obtain text features and calculate the cosine similarity between them. When the score is low enough, we consider the two captions to be different.

3.4.4 Stage2: Difference Captions Generating. In Stage2, for each valid bounding box of each image pair, we first draw two red boxes into the images based on the bounding box information, highlighting the differences for easier localization. Then, we provide the MLLM LLaVA-NEXT with the captions of the bounding box regions and instruct it to describe the differences based on the content captions and the highlighted images. Finally, we can obtain the difference caption for the bounding box of the image pair.

3.5 Data Statistics

In a nutshell, we generate 118K pairs of similar images using captions from MSCOCO and employ the Image Similarity Filter to get 38,533 highly similar but not identical image pairs. Then, we use the Difference Area Generator to filter and produce 117,779

pieces of valid bounding box information (with a maximum of 5 valid bounding boxes per image pair). Finally, we employ the Difference Captions Generator to filter and generate 12,688 high-quality “object replacement” instances.

4 Evaluation on Models trained with IMG-DIFF

4.1 Overview

To evaluate the effectiveness of our IMG-DIFF dataset, we use our dataset to finetune the widely used MLLM LLaVA-1.5[39] and MGM[35], then evaluate them on extensive benchmarks commonly used for image difference and MLLMs. Specifically, the image difference benchmarks include the MMVP[59] benchmark, the Spot-the-Diff[23] benchmark, and the Image-Edit-Request[58] benchmark.

Regarding the finetuning strategy, we mix our data with the original visual instruction tuning dataset of LLaVA-1.5 and MGM respectively and conduct finetuning to get the finetuned MLLMs. For Spot-the-Diff and Image-Edit-Request, since there are training splits in their datasets, we further finetune the MLLMs for an additional 2 epochs using only the benchmark’s training data.

In the tables, “RP” represents “object replacement” data. For the image difference benchmarks, we select various SOTA models for comparison based on the original papers of these benchmarks and recent research on image difference captioning models.

4.2 Results on the MMVP Benchmark

The MMVP benchmark is designed to systematically assess the visual capabilities of MLLMs. Its construction method is highly related to differential images: it first collects CLIP-blind pairs, which have similar CLIP features but differ in image content. Then, the differences between the images are manually described and question-answer pairs are created. Hence, the questions in MMVP is highly relevant to our dataset, as both place significant emphasis on the differences between similar images. Figure 5 presents the results on the MMVP benchmark.

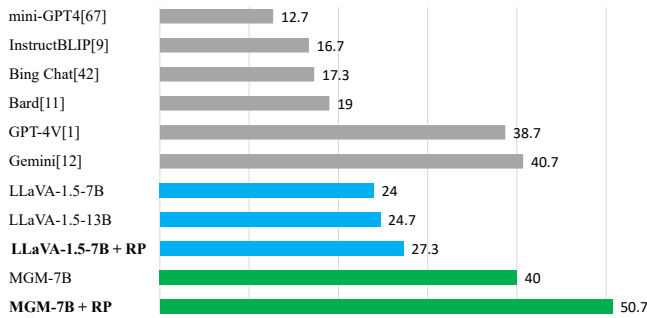


Figure 5: Performance comparison on the MMVP benchmark.

In Figure 5, we can see that finetuning LLaVA-1.5-7B and MGM-7B with our “object replacement” data noticeably improves their performance on the MMVP benchmark. After fine-tuning, the score of LLaVA-1.5-7B surpass that of LLaVA-1.5-13B. Furthermore, the finetuned MGM-7B show a significant improvement in score compared to the original MGM-7B, even exceeding the scores of the

SOTA models GPT-4V and Gemini. This suggests that our dataset enhances the MLLM’s ability to distinguish images with similar CLIP features but different content.

4.3 Results on the Spot-the-Diff Benchmark

The dataset of Spot-the-Diff comprises a collection of street view images. These images are obtained by capturing scenes from fixed surveillance cameras at different time, resulting in pairs of street view images with minor object differences. Following previous works, our finetuned MLLMs are evaluated on BLEU[47], METEOR[4], CIDEr-D[64] and ROUGE-L[36]. Table 1 presents the results on the Spot-the-Diff benchmark.

Table 1: Results on the Spot-the-Diff benchmark.

Model	BLEU	METEOR	CIDEr-D	ROUGE-L
VAM[55]	<u>10.1</u>	12.4	38.1	31.3
IFDC[20]	8.7	11.7	37	30.2
DUDA+Aux[19]	8.1	12.5	34.5	29.9
VACC[27]	9.7	12.6	41.5	<u>32.1</u>
LLaVA-1.5-7B	8.5	12.0	38.3	30.1
LLaVA-1.5-7B+RP	9.7	<u>13.0</u>	43.2	30.8
MGM-7B	9.9	12	46.3	31.5
MGM-7B+RP	10.8	13.1	53.5	33.0

Based on Table 1, it is evident that after finetuning with our “object replacement” data, both LLaVA-1.5-7B and MGM-7B achieve significant performance improvements on the Spot-the-Diff benchmark, which indicates that our dataset enhances the ability of MLLMs to detect subtle differences between similar images.

4.4 Results on Image-Editing-Request

The Image-Editing-Request benchmark is focusing on image editing. Each instance in its dataset consists of an image pair (i.e., a source image and an edited image) and an editing instruction which describes the transformation from the source image to the edited image. During evaluation, our models are required to generate transformation description for these image pairs, and we then calculate the BLEU, METEOR, CIDEr-D, and ROUGE-L scores with the models’ responses and the reference answers. Table 2 presents the results on the Image-Editing-Request benchmark.

Table 2: Results on the Image-Edit-Request benchmark.

Model	BLEU	METEOR	CIDEr-D	ROUGE-L
VARD[61]	10	14.8	35.7	39
CLIP4IDC[15]	8.2	14.6	32.2	40.4
NCT[62]	8.1	15	34.2	38.8
BiDiff[57]	6.9	14.6	27.7	38.5
VIXEN[5]	8.6	15.4	38.1	42.5
LLaVA-1.5-7B	15.1	17.8	60.6	45.2
LLaVA-1.5-7B+RP	16.2	19.5	60.9	46.7
MGM-7B	<u>16.5</u>	17.7	<u>66.8</u>	44.8
MGM-7B+RP	16.6	<u>18.2</u>	68.1	<u>45.7</u>

Table 3: Performance comparison on 8 MLLM benchmarks.

Model	VQA ^{v2}	GQA	POPE	MMB	MMB ^{CN}	MM-Vet	SQA ^I	SEED	Δ
LLaVA-1.5-7B	78.5	62	85.9	64.3	58.3	30.5	66.8	58.6	-
LLaVA-1.5-7B+RP	79.3(+0.8)	62.8(+0.8)	86.4(+0.5)	66.1(+1.8)	59.8(+1.5)	33.2(+2.7)	68.2(+1.4)	61.7(+3.1)	+3.06%
MGM-7B	80.4	62.6	86	69.3	58.9	40.8	70.6	63.5	-
MGM-7B+RP	80.7(+0.3)	62.7(+0.1)	86.2(+0.2)	68.7(-0.6)	59.6(+0.7)	44.1(+3.3)	71.7(+1.1)	63.2(-0.3)	+1.28%

Table 4: The impact of different filtering thresholds on the performance of our dataset.

Threshold	VQA ^{v2}	GQA	POPE	MMB	MMB ^{CN}	MM-Vet	SQA ^I	SEED	Δ
LLaVA-1.5-7B	78.5	62.0	85.9	64.3	58.3	30.5	66.8	58.6	-
(1) IS 0.9-0.98 + BITM 0.3 + CS 0.9 + CITM 0.3	79.1	62.3	86.0	66.8	59.5	32.7	66.6	61.6	+2.42%
(2) IS 0.9-0.98 + BITM 0.35 + CS 0.9 + CITM 0.3	79.1	62.2	85.9	66.7	59.5	32.7	67.1	61.9	+2.52%
(3) IS 0.9-0.98 + BITM 0.35 + CS 0.85 + CITM 0.4	79.3	62.8	86.4	66.1	59.8	33.2	68.2	61.7	+3.06%
(4) IS 0.85-0.98 + BITM 0.35 + CS 0.85 + CITM 0.4	79.2	62.7	86.3	66.2	57.4	32.2	68.8	61.8	+2.24%
(5) IS 0.9-0.98 + BITM ∞ + CS 0.85 + CITM 0.4	79.2	62.3	85.9	66.9	60.0	31.9	68.0	61.3	+2.42%

As shown in Table 2, both LLaVA-1.5-7B and MGM-7B originally show SOTA performance on the Image-Edit-Request benchmark. Upon incorporating our “object replacement” data for further finetuning, the performance of both LLaVA-1.5-7B and MGM-7B improves even more, achieving new SOTA scores. This suggests that our dataset enhances MLLMs’ abilities to recognize similarities and dissimilarities in image pairs and enables them to describe differences more accurately.

4.5 Results on MLLM Benchmarks

Aside from evaluations related to image difference discrimination capabilities, we also assess the performance of our IMG-DIFF dataset in enhancing the comprehensive abilities of MLLMs. We test our dataset using commonly used MLLM benchmarks, including VQAv2[14] and GQA[21] for assessing the comprehensive VQA capabilities of MLLMs; MMBench[42], MM-Vet[68], ScienceQA[43], and SEED-Bench[31] for testing perceptual and reasoning abilities; and POPE[34] for evaluating fine-grained object localization abilities. Table 3 presents the benchmark results on these 8 MLLM benchmarks, with the Δ metric indicating the percentage improvement averaged across them.

Based on Table 3, it can be observed that after finetuning with our dataset, the performance of LLaVA-1.5-7B shows a comprehensive improvement, with an average increase of 3.06% across all benchmarks. For MGM-7B, the improvements brought by our dataset are not as pronounced as those observed with LLaVA-1.5-7B, but it still achieves an average increase of 1.28%. These score improvements indicate that the finetuned MLLMs not only enhance the ability to discern differences but also improve overall visual capabilities, thereby better addressing VQA tasks.

4.6 Ablation Studies

To investigate the impact of filtering thresholds on our data performance, we set different filtering thresholds and generate various versions of our dataset. We then finetune multiple versions of LLaVA-1.5-7B using these datasets and evaluate their performance on commonly used MLLM benchmarks. Specifically, the

filtering threshold for the Image Similarity Filter of the Difference Area Generator is abbreviated as **IS** (Image Similarity). The filtering threshold for the Image-Text Matching Filter of the Difference Area Generator is abbreviated as **BITM** (Bounding Box Image-Text Matching). The filtering threshold for the Caption Similarity Filter of the Difference Captions Generator is abbreviated as **CS** (Captions Similarity). Lastly, the filtering threshold for the Image-Text Matching Filter of the Difference Captions Generator is abbreviated as **CITM** (Captions Image-Text Matching). The evaluation results are shown in Table 4.

Image Similarity (IS). Based on Table 4, Model (3) adjusts the IS threshold from 0.9-0.98 to 0.85-0.98 compared to Model (4), reducing the filtering intensity for the similarity of image pairs. This adjustment leads to a significant performance decline, indicating that the similarity of image pairs has a substantial impact on data quality. When similarity is low, the data generation process may introduce more noise, as semantic segmentation could generate more areas unrelated to the objects being replaced, resulting in ineffective samples.

Bounding Box Image-Text Matching (BITM). Model (2), compared to Model (1), increases the BITM threshold, meaning that when filtering to obtain valid bounding boxes, only those more likely to contain valid objects (i.e., the replaced or replacing objects) are retained. After raising the threshold, slight improvements in model performance are observed. Additionally, Model (5) removes the BITM-related Image-Text Matching filtering compared to Model (3). This operation means that as long as there is any object difference between the areas of the same bounding box of the image pair, the bounding box is considered valid, regardless of whether it contains the valid objects. This operation reduces the filtering intensity, resulting in more instances in our dataset. However, after removing the BITM-related Image-Text Matching filtering, the model’s performance significantly declines. These two experiments demonstrate that higher BITM filtering intensity leads to better model performance, indicating that only bounding boxes related to the replaced or replacing objects should be retained.

Captions Similarity (CS) and Captions Image-Text Matching (CITM). Model (3) increases both the CS threshold and the CITM threshold compared to Model (2). Raising the CS threshold implies a greater filtering strength for similar captions, which means that if the two objects inside the two bounding box areas of an image pair have a certain degree of similarity, the bounding box will be filtered out. Increasing the CITM threshold aims to enhance the alignment between the captions and the objects being described. After raising both the CS and CITM thresholds, the model’s performance shows a significant improvement.

From the results shown in Table 4, it can be concluded that the stronger the filtering intensity, the better our dataset’s effectiveness. However, due to the increased filtering intensity resulting in a reduced number of final instances, we choose the settings of Model (3) as our optimal threshold to ensure a sufficient number of generated instances. In our future work, we plan to expand the data sources to generate more pairs of similar images and then evaluate the effects of data obtained with higher filtering intensity.

5 Evaluation of Data Quality and Diversity

5.1 Data Quality

To assess the quality of our Img-Diff dataset, we randomly select 1,000 instances of “object replacement” data and employ multiple professional dataset annotators to evaluate these samples based on three metrics. The final scores are determined through a voting process. Specifically, the first metric is “**Bounding Box Difference**”, which evaluates whether there are differences between the two sub-images of the same bounding box. If the objects are different, we score it as “high”; if the objects are the same but their features (such as color, shape, etc.) are noticeably different, we score it as “medium”; if the objects are the same and their features are similar, we score it as “low”. The second metric is “**Content Caption Accuracy**”, which evaluates whether the captions generated by Stage 1 of the Difference Captions Generator accurately describe the sub-images. If both captions are correct, we score it as “high”; if the captions identify the objects but incorrectly describe their features, we score it as “medium”; if the captions incorrectly identify the objects, we score it as “low”. The third metric is “**Difference Caption Accuracy**”, which evaluates whether the final difference captions accurately describe the object differences between the image pairs. If the description is accurate, we score it as “high”; if the object recognition is correct but the feature description is incorrect, we score it as “medium”; if the object recognition is incorrect, we score it as “low”. The results are shown in Figure 6.

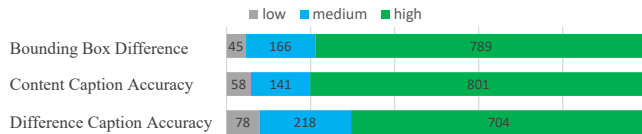


Figure 6: Quality of the “object replacement” data.

Based on Figure 6, our dataset demonstrates a high level of quality. For the “Bounding Box Difference” metric, only 4.5% of the

instances are classified as “low”, and nearly 80% of instances exhibit significant object differences between their two sub-images. In terms of “Content Caption Accuracy”, 80.1% of sub-image pairs are described accurately, indicating that using an MLLM for labeling is effective and that our filtering strategy is also functioning well. For the “Difference Caption Accuracy” metric, over 70% of the difference descriptions are completely accurate, with 21.8% of the samples having errors solely in feature labeling while still maintaining correct descriptions of object differences, which underscores the effectiveness of our difference caption generation strategy.

5.2 Data Diversity

The effectiveness of a dataset is closely related to the diversity of its data. By analyzing the valid object nouns included in the captions of our image pairs, we assess the diversity of our “object replacement” data. Specifically, we count the total number of object categories covered, the total number of unique “object replacement pairs”, and the frequency of occurrences for each object category. The statistical data is presented in Table 5.

Table 5: Diversity of the “object replacement” data.

Categories	Pairs	Total	Avg	Avg _{Obj365}
1,203	3,680	25,288	21.02	36.07

As indicated in Table 5, the number of object categories covered by our dataset is 1,203, encompassing most objects in real life. The term “object replacement pair” refers to the combination of the replaced and replacing object names. The total number of unique “object replacement pairs” covered by our dataset is 3,680, with an average of 3.4 occurrences per pair. The total number of occurrences of object categories in our dataset is 25,288, with an average of 21.02 occurrences per category.

To evaluate the coverage of common object categories in our dataset, we analyze the occurrences of the object categories from the Object365[54] dataset in our own dataset. The results show that each object category from the Object365 dataset appears an average of 36.07 times in our dataset, totaling 13,164 occurrences, which accounts for approximately 52.06% of the total occurrences of object categories. This indicates that our dataset includes a substantial number of common object categories, ensuring a high frequency of these categories. Additionally, less common object categories make up nearly half of our dataset, demonstrating the broad coverage and high diversity of our dataset.

6 The “Object Removal” Exploration

Besides object replacement, determining the presence or absence of objects is also crucial. We generate a new set of data focusing on object removal, which prompts MLLMs to analyze which image in a image pair contains the specific object. Finally, we evaluate this new dataset and find that with this data, the performance improvement for LLaVA-1.5-7B increased to 3.91%, while the improvement for MGM-7B reduced to 1.1%. With these results, we conclude that if MLLMs’ finetuning data is limited and does not include data related to object presence, using “object removal” data can be an option for

data augmentation. Details of “object removal” data are presented in Appendix A.

7 Conclusion

In this paper, we draw inspiration from recent advances in contrastive learning and image difference captioning to propose a novel method of contrastive data synthesis, creating a high-quality dataset called “IMG-DIFF” that focuses on describing object differences. Specifically, we generate many pairs of similar images where the main focus is on object replacement. Then, we use the proposed *Difference Area Generator* and *Difference Captions Generator* to generate difference captions for specific regions and form question-answer pairs. In contrast to previous image difference datasets, our dataset focuses exclusively on specific regions inside the images, circumventing the issue where the descriptive information of differences does not fully capture the differences between image pairs, thereby enhancing the accuracy of the data. Afterwards, we fine-tune LLaVA-1.5-7B and MGM-7B using our relatively small-scale dataset, yielding high performance scores on par with SOTA models trained with much larger-scale datasets in image difference tasks, and comprehensive performance improvements in numerous widely recognized MLLM benchmarks. These results confirm that our dataset effectively improves the ability of MLLMs to recognize differences between images and perform detailed image recognition.

In a nutshell, we provide a series of insights about the construction of high-quality image difference datasets, showing great potential to effectively and efficiently enhance MLLMs via contrastive data-centric approaches. We meticulously detail the process of creating our IMG-DIFF dataset and demonstrate the enhanced performance of MLLMs finetuned with our data on both image difference benchmarks and MLLM benchmarks. With this work, we hope it can catalyze further investigation into the realm of image difference datasets and the fine-grained image recognition capabilities of MLLMs.

References

- [1] Josh Achiam, Steven Adler, Sandhini Agarwal, Lama Ahmad, Ilge Akkaya, Florencia Leoni Aleman, Diogo Almeida, Janko Altmenschmidt, Sam Altman, Shyamal Anadkat, et al. 2023. Gpt-4 technical report. *arXiv preprint arXiv:2303.08774* (2023).
- [2] Jean-Baptiste Alayrac, Jeff Donahue, Pauline Luc, Antoine Miech, Iain Barr, Yana Hasson, Karel Lenc, Arthur Mensch, Katherine Millican, Malcolm Reynolds, et al. 2022. Flamingo: a visual language model for few-shot learning. *Advances in Neural Information Processing Systems* 35 (2022), 23716–23736.
- [3] Jinze Bai, Shuai Bai, Shusheng Yang, Shijie Wang, Sinan Tan, Peng Wang, Junyang Lin, Chang Zhou, and Jingren Zhou. 2023. Qwen-vl: A frontier large vision-language model with versatile abilities. *arXiv preprint arXiv:2308.12966* (2023).
- [4] Satantjeet Banerjee and Alon Lavie. 2005. METEOR: An automatic metric for MT evaluation with improved correlation with human judgments. In *Proceedings of the acl workshop on intrinsic and extrinsic evaluation measures for machine translation and/or summarization*. 65–72.
- [5] Alexander Black, Jing Shi, Yifei Fan, Tu Bui, and John Collomosse. 2024. VIXEN: Visual Text Comparison Network for Image Difference Captioning. In *Proceedings of the AAAI Conference on Artificial Intelligence*, Vol. 38. 846–854.
- [6] Tim Brooks, Aleksander Holynski, and Alexei A Efros. 2023. Instructpix2pix: Learning to follow image editing instructions. In *Proceedings of the IEEE/CVF Conference on Computer Vision and Pattern Recognition*. 18392–18402.
- [7] Daoyuan Chen, Yilun Huang, Zhijian Ma, Heseng Chen, Xuchen Pan, Ce Ge, Dawei Gao, Yuexiang Xie, Zhaoyang Liu, Jinyang Gao, et al. 2024. Data-juicer: A one-stop data processing system for large language models. In *Companion of the 2024 International Conference on Management of Data*. 120–134.
- [8] Daoyuan Chen, Haibin Wang, Yilun Huang, Ce Ge, Yaliang Li, Bolin Ding, and Jingren Zhou. 2024. Data-Juicer Sandbox: A Comprehensive Suite for Multimodal Data-Model Co-development. *arXiv preprint arXiv:2407.11784* (2024).
- [9] Keqin Chen, Zhao Zhang, Weili Zeng, Richong Zhang, Feng Zhu, and Rui Zhao. 2023. Shikra: Unleashing Multimodal LLM’s Referential Dialogue Magic. *arXiv preprint arXiv:2306.15195* (2023).
- [10] Wei-Lin Chiang, Zhuohan Li, Zi Lin, Ying Sheng, Zhanghao Wu, Hao Zhang, Lianmin Zheng, Siyuan Zhuang, Yonghao Zhuang, Joseph E Gonzalez, et al. 2023. Vicuna: An open-source chatbot impressing gpt-4 with 90%* chatgpt quality. See <https://vicuna.lmsys.org> (accessed 14 April 2023) (2023).
- [11] W Dai, J Li, D Li, AMH Tiong, J Zhao, W Wang, B Li, P Fung, and S Hoi. 2023. InstructBLIP: Towards General-purpose Vision-Language Models with Instruction Tuning. *arXiv preprint arXiv:2305.06500* (2023).
- [12] Alexey Dosovitskiy, Lucas Beyer, Alexander Dehghani, Dirk Weissenborn, Xiuhua Zhai, Thomas Unterthiner, Mostafa Dehghani, Matthias Minderer, Georg Heigold, Sylvain Gelly, et al. 2020. An image is worth 16x16 words: Transformers for image recognition at scale. *arXiv preprint arXiv:2010.11929* (2020).
- [13] Google. 2023. Gemini. (2023).
- [14] Yash Goyal, Tejas Khot, Douglas Summers-Stay, Dhruv Batra, and Devi Parikh. 2017. Making the v in vqa matter: Elevating the role of image understanding in visual question answering. In *Proceedings of the IEEE conference on computer vision and pattern recognition*. 6904–6913.
- [15] Zixin Guo, Tzu-Jui Julius Wang, and Leena Laaksonen. 2022. CLIP4IDC: CLIP for image difference captioning. *arXiv preprint arXiv:2206.00629* (2022).
- [16] Kaiming He, Xiangyu Zhang, Shaoqing Ren, and Jian Sun. 2016. Deep residual learning for image recognition. In *Proceedings of the IEEE conference on computer vision and pattern recognition*. 770–778.
- [17] Amir Hertz, Ron Mokady, Jay Tenenbaum, Kfir Aberman, Yael Pritch, and Daniel Cohen-Or. 2022. Prompt-to-Prompt Image Editing with Cross Attention Control. *arXiv preprint arXiv:2208.01626* (2022).
- [18] Sepp Hochreiter and Jürgen Schmidhuber. 1997. Long short-term memory. *Neural computation* 9, 8 (1997), 1735–1780.
- [19] Mehrdad Hosseinzadeh and Yang Wang. 2021. Image change captioning by learning from an auxiliary task. In *Proceedings of the IEEE/CVF Conference on Computer Vision and Pattern Recognition*. 2725–2734.
- [20] Qingbao Huang, Yu Liang, Jielong Wei, Yi Cai, Hanyu Liang, Ho-fung Leung, and Qing Li. 2021. Image difference captioning with instance-level fine-grained feature representation. *IEEE transactions on multimedia* 24 (2021), 2004–2017.
- [21] Drew A Hudson and Christopher D Manning. 2019. Gqa: A new dataset for real-world visual reasoning and compositional question answering. In *Proceedings of the IEEE/CVF conference on computer vision and pattern recognition*. 6700–6709.
- [22] Laurençon Hugo, van Strien Daniel, Bekman Stas, Tronchon Leo, Saulnier Lucile, Wang Thomas, Karamcheti Siddharth, Singh Amanpreet, Pistilli Giada, Jernite Yacine, and Sanh Victor. 2023. Introducing IDEFICS: An Open Reproduction of State-of-the-Art Visual Language Model. <https://huggingface.co/blog/idefics>.
- [23] Harsh Jhamtani and Taylor Berg-Kirkpatrick. 2018. Learning to describe differences between pairs of similar images. *arXiv preprint arXiv:1808.10584* (2018).
- [24] Qirui Jiao, Daoyuan Chen, Yilun Huang, Yaliang Li, and Ying Shen. 2024. Enhancing multimodal large language models with vision detection models: An empirical study. *arXiv preprint arXiv:2401.17981* (2024).
- [25] Glenn Jocher, Ayush Chaurasia, and Jing Qiu. 2023. Ultralytics YOLO. <https://github.com/ultralytics/ultralytics>
- [26] Sahar Kazemzadeh, Vicente Ordonez, Mark Matten, and Tamara Berg. 2014. Referitgame: Referring to objects in photographs of natural scenes. In *Proceedings of the 2014 conference on empirical methods in natural language processing (EMNLP)*. 787–798.
- [27] Hoesong Kim, Jongseok Kim, Hyungseok Lee, Hyunsung Park, and Gunhee Kim. 2021. Agnostic change captioning with cycle consistency. In *Proceedings of the IEEE/CVF International Conference on Computer Vision*. 2095–2104.
- [28] Alexander Kirillov, Eric Mintun, Nikhila Ravi, Hanzi Mao, Chloe Rolland, Laura Gustafson, Tete Xiao, Spencer Whitehead, Alexander C Berg, Wan-Yen Lo, et al. 2023. Segment anything. In *Proceedings of the IEEE/CVF International Conference on Computer Vision*. 4015–4026.
- [29] Ranjay Krishna, Yuke Zhu, Oliver Groth, Justin Johnson, Kenji Hata, Joshua Kravitz, Stephanie Chen, Yannis Kalantidis, Li-Jia Li, David A Shamma, et al. 2017. Visual genome: Connecting language and vision using crowdsourced dense image annotations. *International journal of computer vision* 123 (2017), 32–73.
- [30] Hugo Laurençon, Léo Tronchon, Matthieu Cord, and Victor Sanh. 2024. What matters when building vision-language models? *arXiv preprint arXiv:2405.02246* (2024).
- [31] Bohao Li, Rui Wang, Guangzhi Wang, Yuying Ge, Yixiao Ge, and Ying Shan. 2023. Seed-bench: Benchmarking multimodal llms with generative comprehension. *arXiv preprint arXiv:2307.16125* (2023).
- [32] Junnan Li, Dongxu Li, Silvio Savarese, and Steven Hoi. 2023. Blip-2: Bootstrapping language-image pre-training with frozen image encoders and large language models. *arXiv preprint arXiv:2301.12597* (2023).
- [33] Junnan Li, Dongxu Li, Caiming Xiong, and Steven Hoi. 2022. Blip: Bootstrapping language-image pre-training for unified vision-language understanding and generation. In *International conference on machine learning*. PMLR, 12888–12900.
- [34] Yifan Li, Yifan Du, Kun Zhou, Jinpeng Wang, Wayne Xin Zhao, and Ji-Rong Wen. 2023. Evaluating object hallucination in large vision-language models. *arXiv preprint arXiv:2305.10355* (2023).
- [35] Yanwei Li, Yuechen Zhang, Chengyao Wang, Zhisheng Zhong, Yixin Chen, Ruihang Chu, Shaoteng Liu, and Jiaya Jia. 2023. Mini-Gemini: Mining the Potential of Multi-modality Vision Language Models. *arXiv:2403.18814* (2023).
- [36] Chin-Yew Lin. 2004. Rouge: A package for automatic evaluation of summaries. In *Text summarization branches out*. 74–81.
- [37] Tsung-Yi Lin, Michael Maire, Serge Belongie, James Hays, Pietro Perona, Deva Ramanan, Piotr Dollár, and C Lawrence Zitnick. 2014. Microsoft coco: Common objects in context. In *Computer Vision—ECCV 2014: 13th European Conference, Zurich, Switzerland, September 6–12, 2014, Proceedings, Part V 13*. Springer, 740–755.
- [38] Ziyi Lin, Chris Liu, Renrui Zhang, Peng Gao, Longtian Qiu, Han Xiao, Han Qiu, Chen Lin, Wenqi Shao, Keqin Chen, et al. 2023. Sphinx: The joint mixing of weights, tasks, and visual embeddings for multi-modal large language models. *arXiv preprint arXiv:2311.07575* (2023).
- [39] Haotian Liu, Chunyuan Li, Yuheng Li, and Yong Jae Lee. 2023. Improved Baselines with Visual Instruction Tuning.
- [40] Haotian Liu, Chunyuan Li, Yuheng Li, Bo Li, Yuanhan Zhang, Sheng Shen, and Yong Jae Lee. 2024. LLaVA-NeXT: Improved reasoning, OCR, and world knowledge. <https://llava-vl.github.io/blog/2024-01-30-llava-next/>
- [41] Haotian Liu, Chunyuan Li, Qingyang Wu, and Yong Jae Lee. 2023. Visual instruction tuning. *arXiv preprint arXiv:2304.08485* (2023).
- [42] Yuan Liu, Haodong Duan, Yuanhan Zhang, Bo Li, Songyang Zhang, Wangbo Zhao, Yike Yuan, Jiaqi Wang, Conghui He, Ziwei Liu, et al. 2023. Mmbench: Is your multi-modal model an all-around player? *arXiv preprint arXiv:2307.06281* (2023).
- [43] Pan Lu, Swaroop Mishra, Tanglin Xia, Liang Qiu, Kai-Wei Chang, Song-Chun Zhu, Oyvind Tafjord, Peter Clark, and Ashwin Kalyan. 2022. Learn to explain: Multimodal reasoning via thought chains for science question answering. *Advances in Neural Information Processing Systems* 35 (2022), 2507–2521.
- [44] Gen Luo, Yiyi Zhou, Tianhe Ren, Shengxin Chen, Xiaoshuai Sun, and Rongrong Ji. 2023. Cheap and quick: Efficient vision-language instruction tuning for large language models. *arXiv preprint arXiv:2305.15023* (2023).
- [45] Ben Mann, N Ryder, M Subbiah, J Kaplan, P Dhariwal, A Neelakantan, P Shyam, G Sastry, A Askell, S Agarwal, et al. 2020. Language models are few-shot learners. *arXiv preprint arXiv:2005.14165* 1 (2020).
- [46] Anand Mishra, Shashank Shekhar, Ajeet Kumar Singh, and Anirban Chakraborty. 2019. Ocr-vqa: Visual question answering by reading text in images. In *2019 international conference on document analysis and recognition (ICDAR)*. IEEE, 947–952.
- [47] Kishore Papineni, Salim Roukos, Todd Ward, and Wei-Jing Zhu. 2002. Bleu: a method for automatic evaluation of machine translation. In *Proceedings of the 40th annual meeting of the Association for Computational Linguistics*. 311–318.
- [48] Dong Huk Park, Trevor Darrell, and Anna Rohrbach. 2019. Robust change captioning. In *Proceedings of the IEEE/CVF International Conference on Computer Vision*. 4624–4633.

- [49] Dustin Podell, Zion English, Kyle Lacey, Andreas Blattmann, Tim Dockhorn, Jonas Müller, Joe Penna, and Robin Rombach. 2023. Sdxl: Improving latent diffusion models for high-resolution image synthesis. *arXiv preprint arXiv:2307.01952* (2023).
- [50] Zhen Qin, Daoyuan Chen, Wenhao Zhang, Liuyi Yao, Yilun Huang, Bolin Ding, Yaliang Li, and Shuiguang Deng. 2024. The Synergy between Data and Multi-Modal Large Language Models: A Survey from Co-Development Perspective. *arXiv preprint arXiv:2407.08583* (2024).
- [51] Alec Radford, Jong Wook Kim, Chris Hallacy, Aditya Ramesh, Gabriel Goh, Sandhini Agarwal, Girish Sastry, Amanda Askell, Pamela Mishkin, Jack Clark, et al. 2021. Learning transferable visual models from natural language supervision. In *International conference on machine learning*. PMLR, 8748–8763.
- [52] Robin Rombach, Andreas Blattmann, Dominik Lorenz, Patrick Esser, and Björn Ommer. 2022. High-Resolution Image Synthesis With Latent Diffusion Models. In *Proceedings of the IEEE/CVF Conference on Computer Vision and Pattern Recognition (CVPR)*. 10684–10695.
- [53] Axel Sauer, Dominik Lorenz, Andreas Blattmann, and Robin Rombach. 2023. Adversarial diffusion distillation. *arXiv preprint arXiv:2311.17042* (2023).
- [54] Shuai Shao, Zeming Li, Tianyuan Zhang, Chao Peng, Gang Yu, Xiangyu Zhang, Jing Li, and Jian Sun. 2019. Objects365: A large-scale, high-quality dataset for object detection. In *Proceedings of the IEEE/CVF international conference on computer vision*. 8430–8439.
- [55] Xiangxi Shi, Xu Yang, Jiuxiang Gu, Shafiq Joty, and Jianfei Cai. 2020. Finding it at another side: A viewpoint-adapted matching encoder for change captioning. In *Computer Vision—ECCV 2020: 16th European Conference, Glasgow, UK, August 23–28, 2020, Proceedings, Part XIV 16*. Springer, 574–590.
- [56] Amanpreet Singh, Vivek Natarajan, Meet Shah, Yu Jiang, Xinlei Chen, Dhruv Batra, Devi Parikh, and Marcus Rohrbach. 2019. Towards vqa models that can read. In *Proceedings of the IEEE/CVF conference on computer vision and pattern recognition*. 8317–8326.
- [57] Yaoqi Sun, Liang Li, Tingting Yao, Tongyu Lu, Bolun Zheng, Chenggang Yan, Hua Zhang, Yongjun Bao, Guiguang Ding, and Gregory Slabaugh. 2022. Bidirectional difference locating and semantic consistency reasoning for change captioning. *International Journal of Intelligent Systems* 37, 5 (2022), 2969–2987.
- [58] Hao Tan, Franck Dernoncourt, Zhe Lin, Trung Bui, and Mohit Bansal. 2019. Expressing visual relationships via language. *arXiv preprint arXiv:1906.07689* (2019).
- [59] Shengbang Tong, Zhuang Liu, Yuexiang Zhai, Yi Ma, Yann LeCun, and Saining Xie. 2024. Eyes wide shut? exploring the visual shortcomings of multimodal llms. In *Proceedings of the IEEE/CVF Conference on Computer Vision and Pattern Recognition*. 9568–9578.
- [60] Hugo Touvron, Thibaut Lavril, Gautier Izacard, Xavier Martinet, Marie-Anne Lachaux, Timothée Lacroix, Baptiste Rozière, Naman Goyal, Eric Hambro, Faisal Azhar, et al. 2023. Llama: Open and efficient foundation language models. *arXiv preprint arXiv:2302.13971* (2023).
- [61] Yunbin Tu, Liang Li, Li Su, Junping Du, Ke Lu, and Qingming Huang. 2023. Adaptive representation disentanglement network for change captioning. *IEEE Transactions on Image Processing* 32 (2023), 2620–2635.
- [62] Yunbin Tu, Liang Li, Li Su, Ke Lu, and Qingming Huang. 2023. Neighborhood contrastive transformer for change captioning. *IEEE Transactions on Multimedia* 25 (2023), 9518–9529.
- [63] Ashish Vaswani, Noam Shazeer, Niki Parmar, Jakob Uszkoreit, Llion Jones, Aidan N Gomez, Lukasz Kaiser, and Illia Polosukhin. 2017. Attention is all you need. *Advances in neural information processing systems* 30 (2017).
- [64] Ramakrishna Vedantam, C Lawrence Zitnick, and Devi Parikh. 2015. Cider: Consensus-based image description evaluation. In *Proceedings of the IEEE conference on computer vision and pattern recognition*. 4566–4575.
- [65] Catherine Wah, Steve Branson, Peter Welinder, Pietro Perona, and Serge Belongie. 2011. The caltech-ucsd birds-200-2011 dataset. (2011).
- [66] Weiyun Wang, Min Shi, Qingyun Li, Wenhao Wang, Zhenhang Huang, Linjie Xing, Zhe Chen, Hao Li, Xizhou Zhu, Zhiguo Cao, et al. 2023. The All-Seeing Project: Towards Panoptic Visual Recognition and Understanding of the Open World. In *The Twelfth International Conference on Learning Representations*.
- [67] Shiyu Xuan, Qingpei Guo, Ming Yang, and Shiliang Zhang. 2023. Pink: Unveiling the Power of Referential Comprehension for Multi-modal LLMs. *arXiv preprint arXiv:2310.00582* (2023).
- [68] Weihao Yu, Zhengyuan Yang, Linjie Li, Jianfeng Wang, Kevin Lin, Zicheng Liu, Xinchao Wang, and Lijuan Wang. 2023. Mm-vet: Evaluating large multimodal models for integrated capabilities. *arXiv preprint arXiv:2308.02490* (2023).
- [69] Hao Zhang, Feng Li, Shilong Liu, Lei Zhang, Hang Su, Jun Zhu, Lionel M Ni, and Heung-Yeung Shum. 2022. Dino: Detr with improved denoising anchor boxes for end-to-end object detection. *arXiv preprint arXiv:2203.03605* (2022).
- [70] Renrui Zhang, Jiaming Han, Aojun Zhou, Xiangfei Hu, Shilin Yan, Pan Lu, Hongsheng Li, Peng Gao, and Yu Qiao. 2023. Llama-adaptor: Efficient fine-tuning of language models with zero-init attention. *arXiv preprint arXiv:2303.16199* (2023).
- [71] Xu Zhao, Wenchao Ding, Yongqi An, Yinglong Du, Tao Yu, Min Li, Ming Tang, and Jinqiao Wang. 2023. Fast segment anything. *arXiv preprint arXiv:2306.12156* (2023).

Appendix

A The “Object Removal” Exploration

A.1 Overview

In the main page, we generate many pairs of similar images focusing on object replacement. Their bounding box regions generally contain objects. However, the ability to determine the object presence is also crucial. Thus, we generate another set of pairs of similar images where the difference lies in the presence or absence of objects, to enhance the model’s ability to determine object presence. We refer to these image pairs as “exist-absent pairs” and the data as “object removal” data.

A.2 Generation Process

A.2.1 Workflow. “Object removal” involves erasing a specific object from an image and then merging the edited image with the original to form an exist-absent pair. The detailed workflow is as follows: first, FastSAM is used to segment the image, which provides a set of bounding boxes and masks. Next, the Image Similarity Filter is applied to filter the bounding boxes and accompanying masks, keeping only those that contain objects. Then, we use the text-to-image generative model SDXL-turbo[53] to inpaint the images with the remaining masks, erasing specific objects from the images and generating exist-absent pairs. Afterward, we use an MLLM to describe the removed object for each exist-absent pair, and a filter is employed to verify the accuracy of the description. Finally, we draw red boxes on images based on the bounding box information and then the object descriptions are converted into multiple-choice questions, such as: “*which image has the object related to ‘DESCRIPTION’ within the red bounding box? A. the left image B. the right image.*” Here, *DESCRIPTION* refers to the description of the erased objects. After all processing and filtering, we obtain 5,773 pieces of “object removal” data. The general framework is shown in Figure 7.

A.2.2 Image Similarity Filter. The structure of the current Image Similarity Filter is identical to the one shown in Figure 3. In the current process, the function of the Image Similarity Filter is to filter out bounding boxes whose corresponding areas do not contain objects. For each image, we need its corresponding image in the image pair generated in Section 3.2 to determine whether its bounding box regions contain objects. Since the image pairs are generated by replacing objects, the difference areas between the two images are highly likely to be the regions containing valid objects. Therefore, for each bounding box, we crop the sub-images from image A (the current image) and image B (the other image in the pair), and then calculate the similarity of these two sub-images. When the similarity is below 0.9, we consider these two sub-images to be different, indicating that the bounding box region contains an object.

A.2.3 Erase objects. We use the model SDXL-turbo[53] to erase objects based on the masks obtained during segmentation. The prompt is “background, nothing, 8k.” After inpainting, the object in the masked regions is erased, while the rest of the image remains unchanged. Hence, we obtain exist-absent pairs.

A.2.4 MLLM Captioning. We use the MLLM LLaVA-NEXT to generate descriptions for the erased objects. Specifically, we provide the

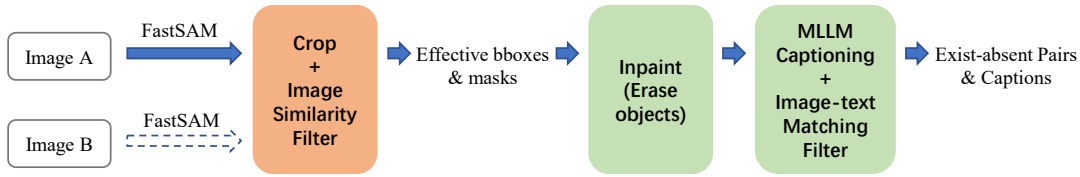


Figure 7: An overview of the generation steps for “object removal” data.

Table 6: Performance comparison on 8 MLLM benchmarks (including “object removal” data).

Model	VQA ^{v2}	GQA	POPE	MMB	MMB ^{CN}	MM-Vet	SQA ^I	SEED	Δ
LLaVA-7B	78.5	62.0	85.9	64.3	58.3	30.5	66.8	58.6	-
LLaVA-7B+RP	79.3	<u>62.8</u>	<u>86.4</u>	66.1	59.8	33.2	68.2	61.7	+3.06%
LLaVA-7B+RP+RM	79.2	62.9	86.8	67.9	61.3	33.1	68.8	61.9	+3.91%
MGM-7B	<u>80.4</u>	62.6	86.0	<u>69.3</u>	58.9	40.8	70.6	63.5	-
MGM-7B+RP	80.7	62.7	86.2	68.7	59.6	44.1	71.7	<u>63.2</u>	+1.28%
MGM-7B+RP+RM	80.2	62.0	<u>86.4</u>	70.5	<u>60.6</u>	<u>43.1</u>	<u>71.2</u>	62.5	+1.10%

Table 7: Results on image difference benchmarks (including “object removal” data).

Model	MMVP	Spot-the-Diff				Image-Edit-Request			
		BLEU	METEOR	CIDEr-D	ROUGE-L	BLEU	METEOR	CIDEr-D	ROUGE-L
LLaVA-1.5-7B	24.0	8.5	12.0	38.3	30.1	15.1	17.8	60.6	45.2
LLaVA-1.5-7B+RP	27.3	9.7	<u>13.0</u>	43.2	30.8	16.2	19.5	60.9	46.7
LLaVA-1.5-7B+RP+RM	28.7	9.8	<u>13.0</u>	<u>46.5</u>	31.5	16.8	<u>18.6</u>	63.9	<u>45.7</u>
MGM-7B	<u>40.0</u>	<u>9.9</u>	12.0	46.3	<u>31.5</u>	16.5	17.7	<u>66.8</u>	44.8
MGM-7B+RP	50.7	10.8	13.1	53.5	33.0	<u>16.6</u>	18.2	68.1	<u>45.7</u>
MGM-7B+RP+RM	37.3	9.1	12.0	43.5	31.1	16.1	17.5	64.1	45.5

MLLM with the bounding box coordinate and ask it to describe the corresponding area in the original image. Subsequently, we crop the exist-absent pairs based on the bounding box information and then use the Image-Text Matching Filter to assess the matching degree between the sub-images and descriptions. If the score between the sub-image containing objects and its description is greater than 0.35, and the score between the sub-image not containing objects and its description is less than 0.2, we consider the description to be accurate and the exist-absent pair to be valid.

A.3 Evaluation

We merge the “object removal” data with the “object replacement” data, making our dataset focus on object changes as well as object presence. To test the performance changes of LLaVA-1.5-7B and MGM-7B after adding “object removal” data, we incorporate the combined data into the original training datasets of these two MLLMs for visual instruction tuning and evaluate the finetuned MLLMs on image difference benchmarks and MLLM benchmarks, just like the main page.

In the tables, “RM” represents “object removal” data.

A.3.1 Results on MLLM benchmarks. Table 6 shows the performance of LLaVA-1.5-7B and MGM-7B finetuned with additional “object removal” data on commonly used MLLM benchmarks. With

the assistance of “object removal” data, LLaVA-1.5-7B achieves further improvements across various benchmarks compared to the model that only includes “object replacement” data, with an average increase of 3.91%. However, after adding “object removal” data, MGM-7B experiences a slight decline in performance, with an average increase of only 1.10% across all the benchmarks. Nevertheless, it still shows score improvements on the POPE benchmark and the MMBench benchmarks.

A.3.2 Results on image difference benchmarks. Table 7 shows the performance of LLaVA-1.5-7B and MGM-7B finetuned with our “object removal” data on image difference benchmarks. It can be observed that with “object removal” data, LLaVA-1.5-7B’s scores improve on the MMVP benchmark and the Spot-the-Diff benchmark, while its scores fluctuate on the Image-Edit-Request benchmark. However, MGM-7B experiences varying degrees of score decreases across all three image difference benchmarks.

A.3.3 Analysis. The benchmark results indicate that the “object removal” data has a comprehensive positive effect on LLaVA-1.5-7B. However, upon finetuning with the “object removal” data, the performance of MGM-7B shows fluctuations. We speculate that the limited improvement for MGM might be due to the broad scope of MGM’s original data, which may already encompass the new

information introduced by our “object removal” dataset. In conclusion, adding “object removal” data does not necessarily lead to a significant performance improvement for MLLMs. However, when finetuning data is limited or does not include data related to the presence or absence of objects, “object removal” data can serve as an option for data augmentation.

B Additional Details of Experiments

B.1 Preprocessing of image pairs before inputting into MLLMs

The MLLMs selected in our paper (LLaVA-1.5, LLaVA-NEXT and MGM) only support single-image input. Therefore, our image pairs need to be horizontally concatenated before being fed into MLLMs’ image encoder. Specifically, we horizontally concatenate the image pair and add a vertical black dividing line, 20 pixels wide, between the images.

B.2 Model Selection

B.2.1 Overview. The models used in our project are among the best-performing ones identified for the tasks assigned to them. Besides, they are interchangeable. Therefore, if better model options become available, researchers can replace the current models with those that offer superior performance to achieve a more effective dataset.

B.2.2 Selection of the Semantic Segmentation Model. In our project, we need to use a semantic segmentation model to identify regions in images that may contain objects. To ensure a diverse range of object categories is covered, we opt for models like SAM[28] instead of traditional semantic segmentation models. Furthermore, to reduce time consumption, we select FastSAM, one of the most efficient and effective models within SAM-like category, as our segmentation model.

B.2.3 Model Size. Considering the device limitation and time consumption, our paper utilizes the LLM Vicuna-1.5-13B for object name replacement in the image pairs generation process. For semantic segmentation in the Difference Area Generator, the FastSAM-x model is employed. For the CLIP model, we choose “clip-vit-base-patch32”, and for the BLIP model, we select “blip-itm-large-coco”. In the Difference Captions Generator, we use the MLLM LLaVA-NEXT-13B to generate content captions and difference captions. These models are interchangeable. When resources allow, researchers can substitute them with higher-performance models to achieve datasets with improved performance.

B.3 Filtering Thresholds

During the generation process of “object replacement” data, we employ multiple filtering operations. In this subsection, we outline the filtering thresholds we use.

In the Difference Area Generator, we use FastSAM to perform semantic segmentation on images and obtain bounding box information for regions where objects might be present. To ensure we gather a sufficient number of candidate regions, we set the confidence score threshold to 0.05, which means that we consider a region to contain objects when its confidence score is greater

than 0.05. Additionally, to prevent overlapping regions, we set the Intersection over Union (IoU) threshold to 0.5.

At the beginning stage of the Difference Area Generator, before using FastSAM for segmentation, we employ the Image Similarity Filter to retain only those with similarity between 0.9 and 0.98. This ensures that the image pairs are highly similar but not identical.

In the Difference Detector stage of the Difference Area Generator, after cropping sub-images based on the bounding box information, we use the Image Similarity Filter to filter the sub-image pairs and consider them to be different only when the similarity score is less than 0.85.

In the mid-stage of the Difference Area Generator, after performing sub-image cropping based on the bounding box information, we use the Image-text Matching Filter to determine whether these sub-images contain valid objects. When the score exceeds 0.35, we consider the sub-image to contain valid objects, and the bounding box is deemed effective.

In the Difference Area Generator, after obtaining all effective bounding boxes, we use the IoU method to filter out overlapping bounding boxes. We set the IoU threshold to 0.5, retaining only the bounding boxes with a higher degree of difference for similar positions.

In stage 1 of the Difference Captions Generator, after cropping the images into sub-images and generating content captions, we use the Image-text matching filter to evaluate the matching degree between the sub-images and the content captions. We only consider a caption to be correct if the image-text matching score exceeds 0.4.

In stage 1 of the Difference Captions Generator, we use the Captions Similarity Filter to determine whether the two content captions of an image pair, describing the regions of the same bounding box, are different. We use CLIP to obtain text features for the two captions and then calculate the cosine similarity between them. When the cosine similarity is below 0.85, we consider the two captions to be different.

Setting the filtering intensity too high may lead to a reduced number of remaining samples. To ensure that the dataset still has enough samples after filtering, we outline adjustable thresholds as described above. As mentioned in Section 4.6, higher filtering intensity typically results in better model performance. Therefore, researchers may consider expanding the data sources and increasing the filtering intensity to improve dataset performance.

C Examples

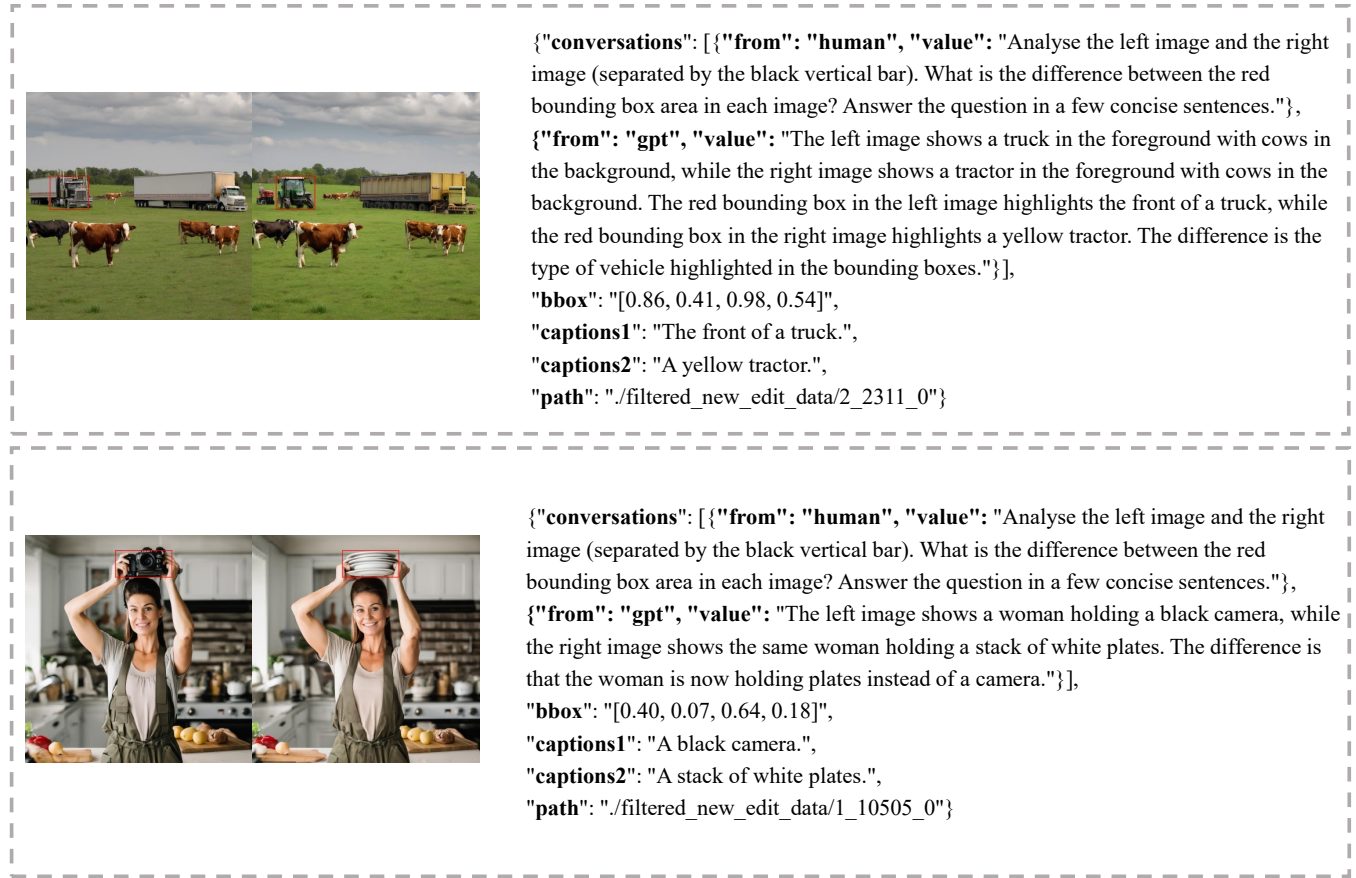


Figure 8: Examples of “object replacement” data, including the image pair and the text content in JSON format.

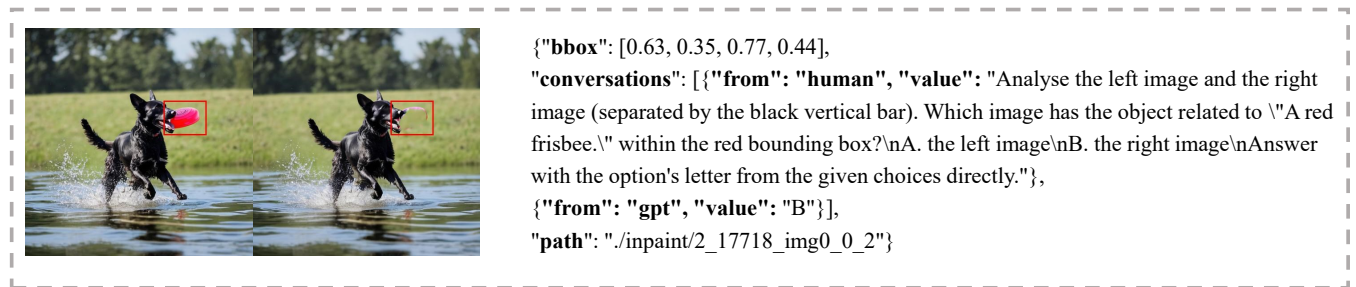


Figure 9: An example of “object removal” data, including the image pair and the text content in JSON format.